

THERMOFORMING PROCESS SIMULATION OF STRETCHABLE ELECTRONIC CIRCUIT

By:

NUR AMIRAH BINTI ISMAIL

(Matrix no: 125040)

Supervisor:

Dr. Abdullah Aziz Saad

MAY 2018

This dissertation is submitted to
Universiti Sains Malaysia
As partial fulfillment of the requirement to graduate with honors degrees in
BACHELOR OF ENGINEERING (MECHANICAL ENGINEERING)



School of Mechanical Engineering
Engineering Campus
Universiti Sains Malaysia

DECLARATION

This work has not previously been accepted in substance for any degree and is not being concurrently submitted in candidature for any degree.

Signed.....

(NUR AMIRAH BINTI ISMAIL)

Date

Statement 1

This thesis is the result of my own investigation, except where otherwise stated. Other sources are acknowledged by giving explicit references. Bibliography/references are appended.

Signed.....

(NUR AMIRAH BINTI ISMAIL)

Date

Statement 2

I hereby give consent for my thesis, if accepted, to be available for photocopying and for interlibrary loan, and for the title and summary to be made available outside organizations.

Signed.....

(NUR AMIRAH BINTI ISMAIL)

Date

ACKNOWLEDGEMENT

I would like to express my deepest gratitude to my supervisor, Dr. Abdullah Aziz Saad for his guidance, advice and help throughout the whole project. I am very thankful for the suggestions and ideas that have been given to me to make my project and writing report going smoothly.

It is my radiant sentiment to place on record my best regards, deepest sense of gratitude to technician, Mr. Mohd Ashamuddin Hashim, who is helping me in using Scanning Electron Microscope to measure the thermoformed polycarbonate thickness at the Microscopy & Micro Analysis Laboratory. I would like to acknowledge with much appreciation to a master student, Norhidayah Bt. Abdul Aziz who has offer a lot of help to me in conducting the rheology test.

Next, I would like to thank all the lectures and technical staffs in the School of Mechanical Engineering, Universiti Sains Malaysia for sharing their knowledge on the thesis writing and their area of expertise and give permission to use the required equipment especially computer in CAD Laboratory and necessary materials to make my project run smoothly. Finally, I would like to thank my family and friend for the moral support throughout my project.

Title of thesis: **Thermoforming Process Simulation of Stretchable Electronic Circuit**

Date of submission (Academic year): **23 May 2018**

Candidate (Matrix no.): **Nur Amirah Binti Ismail (125040)**

Name of supervisor: **Dr. Abdullah Aziz Saad**

Table of Contents	
DECLARATION	ii
ACKNOWLEDGEMENT	iii
LIST OF TABLES	vi
LIST OF FIGURES	vii
LIST OF ABBREVIATION	xi
ABSTRAK.....	xii
ABSTRACT.....	xiii
CHAPTER 1	1
INTRODUCTION	1
1.1 BACKGROUND	1
1.2 PROBLEM STATEMENT	5
1.3 OBJECTIVE	5
1.4 SCOPE OF WORK.....	5
1.5 THESIS STRUCTURE.....	6
CHAPTER 2	7
LITERATURE REVIEW	7
2.1 INTRODUCTION	7
2.2 THERMOFORMING PROCESS	7
2.3 PARAMETER EFFECT ON THERMOFORMING PROCESS.....	8
2.4 BEHAVIOUR AND PROPERTIES OF SUBSTRATE MATERIAL	13
2.5 FINITE ELEMENT SIMULATION OF THERMOFORMING PROCESS	16
2.6 RHEOLOGY TEST	19
2.7 STRETCHABLE ELECTRONIC CIRCUIT.....	23
2.8 GRID ANALYSIS	24
2.9 RHEOLOGY TEST	25
2.10 RHEOLOGY PROPERTIES USED IN ANSYS POLYFLOW	28
2.11 SUMMARY	30
CHAPTER 3	31
METHODOLOGY	31
3.1 INTRODUCTION	31
3.2 MATERIAL SELECTION FOR SUBSTRATE.....	31
3.3 SOLIDWORK MODELLING	31
3.4 ANSYS POLYFLOW (BLOW MOLDING).....	35

3.4.1 MOULD.....	38
3.4.2 NATURE OF THE FLOW	39
3.4.3 SUBSTRATE.....	43
3.5 SCANNING ELECTRON MICROSCOPE (SEM) MEASUREMENT	46
3.6 GRID ANALYSIS	48
CHAPTER 4	49
RESULT AND DISCUSSION	49
4.1 INTRODUCTION	49
4.2 EXPERIMENTAL RESULT ON THICKNESS MEASUREMENT	49
4.3 SIMULATION THICKNESS ANALYSIS	51
4.4 COMPARISON OF THICKNESS BETWEEN EXPERIMENT AND SIMULATION RESULT	54
4.5 PARAMETRIC ANALYSIS ON THE SHAPE OF THE MOULD	56
4.6 AREA STRETCH.....	64
4.7 RELATIONSHIP BETWEEN GRID TEST, AREA STRETCH AND THICKNESS.....	67
4.8 SUMMARY	71
CHAPTER 5	72
CONCLUSION.....	72
5.1 CONCLUSION.....	72
5.2 FUTURE WORK AND IMPROVEMENTS.....	73
REFERENCES	74
APPENDICES	76
APPENDIX A.....	76
APPENDIX B.....	84

LIST OF TABLES

Table 3.41: Sizing setup.....	36
Table 3.42: Viscosity and relaxation time of integral viscoelastic model[12].	40
Table 3.43: Specific value is assigned accordingly to its property.....	44
Table 3.44: Material properties of polycarbonate.....	44
Table 3.45: Value of transient iterative parameter.....	45
Table 4.21: The thickness distributions on top surface and wall surface of thermoformed polycarbonate.	50
Table 4.21: The thickness distributions on top surface of thermoformed polycarbonate for sharp edge.	53
Table 4.41: Percentage error of thickness distribution between experimental and simulation result.....	55
Table 4.51: Thickness distributions on critical corner for different shapes of mould.	60
Table 4.52: The thickness distributions on top surface of thermoformed polycarbonate for corner edge (3 mm fillet).	61
Table 4.53: The thickness distributions on top surface of thermoformed polycarbonate for corner edge (4 mm fillet).	62
Table 4.53: Thickness distributions on side wall for different shapes of mould.	62
Table 4.61: Percentage of elongation of thermoformed polycarbonate with and without stretchable circuit.....	66
Table 4.71: Simulation and experimental result of area stretch ratio and thickness.....	70

LIST OF FIGURES

Figure 1.11: Main steps for thermoforming process.[2]	1
Figure 1.12 (a) : 3D-MID circuit with assembled components.[3].....	2
Figure 1.12 (b) : Examples of industrially produced flex-rigid boards (left:Altium) ,(right:Teknoflex)[3]	3
Figure 1.13: (a) The original design of the automotive lighting part (b) 3-D drawing of the original design .[4].....	4
Figure 2.21: Schematic diagram of vacuum-forming process: (a) sheet heating (b) sheet stretching, and (c) sheet cooling.[6].....	7
Figure 2.31: The effects of plug displacement on the product wall thickness distribution[7]...	8
Figure 2.32: Visual representation of plug displacements of (a) 86.5 mm and (b) 76.5 mm showing increased blow-off distance[7].	9
Figure 2.33: The effects of sheet temperature on the product wall thickness distribution[7]. ..	9
Figure 2.34: Microscopy images (X10 magnification) of the lip and denest regions of pots formed at (a) 120°C and (c) 140°C with (b) stacking[7].....	10
Figure 2.35: (a) Flat bottom (b) blunt, and (c) bullet plug (units in mm)[7].	10
Figure 2.36: The effects of plug shape on the product wall thickness distribution[7].....	11
Figure 2.37: Parts formed by (a) plug mould and (b) cavity mould[5].....	12
Figure 2.38 : Thickness distribution of part cross section formed by cavity mould[5].	12
Figure 2.39 shows wall thickness distribution of the plug mould in which the starting sheet thickness was 0.128 inch. The thinnest location of the plug mould is 0.106 inch represents 70.6% of the original thickness.....	13
Figure 2.41: DSC scanning result for (a) PET and (b) PC materials[4].	15
Figure 2.51 : Heat transfer mechanisms[10].....	16
Figure 2.61 (a): AR-G2 (TA-Instruments) rotational rheometer with the used plate-plate geometry[10].....	19
Figure 2.61 (b) : Plate-plate geometry system[10].	20
Figure 2.61: Measurements of the shear viscosity of Polycarbonate at a temperature region of 220 °C to 300°C for Steady state, Cox-Merz and Capillary[10].	21
Figure 2.62: Storage and loss modulus for a wide range of frequency, from 220°C to 330°C[10].	22

Figure 2.71: First thermoforming experiment, using a non-optimized design, inset (right) shows full extension of meanders.[3]	23
Figure 2.81: (a) Dimensional variation measurement of line segment and (b) thickness distribution of the thermoformed substrate[11].	24
Figure 2.91 (a): AR-G2 (TA-Instruments) rotational rheometer with the used plate-plate geometry.	25
Figure 2.91 (b) : Plate-plate geometry system	26
Figure 2.92: Measurements of the shear viscosity of Polycarbonate at a temperature region of 220 °C to 300°C for Steady state, Cox-Merz and Capillary	27
Figure 2.93: Storage and loss modulus for a wide range of frequency, from 220 °C to 330 °C.	28
Figure 2.11: Plot of computed and experimental curves of the rheology properties[12].	29
Figure 2.12: The results from the fitting curve[12].	30
Figure 3.31 (a): An original model of rear lighting part of Proton Saga.	32
Figure 3.31 (b): 3-D drawing of the rear lighting part of Proton Saga by using Solidworks.	32
Figure 3.32(a): Modified mould design from Solidworks with 3 mm fillet corner edge.	33
Figure 3.32(a): Modified mould design from Solidworks with 4 mm fillet corner edge.	33
Figure 3.33 (a): 3-D assembly drawing of the original design with sharp edges.	34
Figure 3.33 (b): 3-D assembly drawing of the modified design with 3 mm fillet corner edges.	34
Figure 3.41: Thin surfaces are applied for each part in Design Modeler.	35
Figure 3.42: Meshed part configurations after triangle method and sizing setup were applied.	36
Figure 3.43: The four defined boundaries condition of the substrate.	37
Figure 3.44: The interface of Polydata setup.	37
Figure 3.45 (a): Mould ramp function	38
Figure 3.45 (b): Mould motion at time 0.6 s.	39
Figure 3.46 : Polydata setup for the flow boundary condition.	40
Figure 3.47 : Polydata setup for the thermal boundary condition.....	41
Figure 3.48 (a) : Inflation pressure imposed ramp function.	41
Figure 3.48 (b) : The fully deformed sheet after inflation pressure imposed ramp function was applied.....	42
Figure 3.49: Output set unit of the system.....	45

Figure 3.51: Scanning Electron Microscope (S-3400N) used to measure the thickness distribution on thermoformed polycarbonate.....	46
Figure 3.52 (a): Thermoformed polycarbonate substrate of the lighting part.....	47
Figure 3.52 (b): Point allocation on the wall surface of thermoformed polycarbonate substrate of the lighting part.....	47
Figure 3.52 (c): Point allocation on the top surface of thermoformed polycarbonate substrate of the lighting part.....	47
Figure 3.53: Thermoformed polycarbonate substrate of the lighting part.	48
Figure 4.21: Thermoformed polycarbonate substrate of lighting part.	49
Figure 4.31: Simulation result on the top surface thickness of polycarbonate substrate.	51
Figure 4.32: Simulation result on the wall surface thickness of polycarbonate substrate.	52
Figure 4.41: Comparison of thickness between experimental and simulation result.	54
Figure 4.51: Thickness distribution of critical points for sharp edge.	56
Figure 4.52: Thickness distributions of side wall for sharp edge.	57
Figure 4.54: Thickness distributions for side wall for corner edge (3 mm fillet).....	58
Figure 4.55: Thickness distributions for critical corner for corner edge (4 mm fillet).....	58
Figure 4.56: Thickness distributions for sidewall for corner edge (4 mm fillet).....	59
Figure 4.57: Graph of critical corner thickness for different shape of mould used.....	60
Figure 4.58: The average thickness distributions for sharp edge and corner edge	63
Figure 4.61: Thermoformed polycarbonate without stretchable circuit.	64
Figure 4.62: Thermoformed polycarbonate with stretchable circuit.	65
Figure 4.63: Contact position of the polycarbonate substrate and mould during thermoforming process.	66
Figure 4.71 (a) : Simulation results of ASR at first side wall.....	67
Figure 4.71 (b) : Simulation results of ASR at second side wall.....	68
Figure 4.71 (c): Simulation of thickness distribution at first side wall.....	68
Figure 4.71 (d): Simulation of thickness distribution at first side wall.	69
Figure 4.72 : Experimental results of (a) ASR and thickness at first side wall and (b) ASR and thickness at second side wall[4].....	70
Figure A 1: Top surface 1 thickness reading.	76
Figure A 2: Top surface 2 thickness reading.	76
Figure A 3: Top surface 3 thickness reading.	77
Figure A 4: Top surface 4 thickness reading.	77
Figure A 5: Top surface 5 thickness reading.	78

Figure A 6: Top surface 6 thickness reading.	78
Figure A 7: Top surface 7 thickness reading.	79
Figure A 8: Top surface 8 thickness reading.	79
Figure A 9: Top surface 9 thickness reading.	80
Figure A 10: Wall surface 10 thickness reading.	80
Figure A 11: Wall surface 11 thickness reading.	81
Figure A 12: Wall surface 12 thickness reading.	81
Figure A 13: Wall surface 13 thickness reading.	82
Figure A 15: Wall surface 15 thickness reading.	82
Figure A 16: Wall surface 16 thickness reading.	83
Figure A 17: Wall surface 17 thickness reading.	83
Figure B 1: Time dependence of the z-velocity (ramp function).....	84
Figure B 2: Modification of a contact problem	84
Figure B 3: Transient iterative parameters value.	85
Figure B 4: Global criteria for contact in adaptive meshing	86
Figure B 5: Adaptive meshing criteria.	87

LIST OF ABBREVIATION

PC	Polycarbonate
PET	Polyethylene Terephthalate
T_g	Glass Transition Temperature
T_c	Crystalline Temperature
T_m	Melting Temperature
PC	Polycarbonate
PET	Polyethylene Terephthalate
SEM	Scanning Electron Microscopy
DSC	Differential Scanning Calorimetry
PCB	Printed Circuit Board
LED	Light Emitting Diode
LDS	Laser Direct Structuring
MID	Moulded Interconnect Device
LDS	Laser Direct Structuring
CAD	Computer Aided Design
ASR	Area Stretch Ratio
CMM	Coordinate Measuring Machine
CNC	Computer Numerical Control
E_a	Arrhenius activation energy
T	Absolute temperature
q	Heat flux
q_c	Temperature independent heat flux
α	Heat convection coefficient
T	Temperature at the boundary
T_α	References temperature for convective heat exchange
σ	Coefficient of radiation
T_σ	References temperature for radiative heat exchange
δ_L	Percentage of dimensional elongation
L_i	Measured distance before deformation
L_j	Distance after deformation

KAJIAN PROSES TERMOPEMBENTUKAN LITAR ELEKTRONIK REGANGAN

ABSTRAK

Termopembuatan adalah proses pembuatan yang terkenal di mana kepingan polimer dipanaskan hingga keadaan lentur pada suhu pembentuk dan dileburkan ke dalam bentuk tertentu dalam acuan dan akhirnya dipotong untuk mendapatkan produk yang boleh digunakan. Proses ini digunakan secara meluas dalam industri kerana proses pembuatannya yang kos efektif. Objektif utama projek ini adalah untuk mengkaji kesan proses dan parameter termopembuatan pada pengagihan ketebalan ke atas produk dengan menggunakan simulasi ANSYS Polyflow. Simulasi ANSYS Polyflow digunakan untuk mengkaji proses keseluruhan termopembentukan untuk menjimatkan masa dan mengurangkan kos yang digunakan untuk menghasilkan sebarang produk prototaip. Acuan dengan bentuk yang berbeza iaitu sudut berbucu dengan 3 mm radius dan sudut tajam digunakan di dalam disimulasi untuk mendapatkan pengagihan ketebalan yang terbaik pada produk. Acuan sudut berbucu dengan 3 mm radius mengurangkan dan mengagihkan tekanan lebih rata pada produk. Oleh itu, nilai ketebalan di sudut dalam (sudut kritikal) telah dikurangkan. Analisis grid dilakukan pada produk termopembuatan dengan dan tanpa litar bercetak di dalamnya. Hasil menunjukkan bahawa filem mengalami perubahan bentuk yang lebih tanpa litar bercetak di atasnya. Pengubahan bentuk filem dengan litar bercetak yang tertanam di atasnya jauh lebih rendah. Bagaimanapun, filem itu dapat berubah bentuk dengan litar bercetak mengikut bentuk acuan. Nisbah regangan kawasan yang lebih besar terdapat di sudut kritikal dan dinding sisi yang rendah. Perubahan bentuk yang lebih tinggi berlaku kerana kedalaman tarikan meningkat. Oleh itu, pengagihan ketebalan dikurangkan dan meningkatkan nisbah regangan kawasan disebabkan kedalaman tarikan meningkat. Kesimpulannya, pemahaman dan teknik mengenai proses termopembentukan pada bahagian lampu kereta telah dicapai.

THERMOFORMING PROCESS STUDY OF STRETCHABLE ELECTRONIC CIRCUIT

ABSTRACT

Thermoforming is a well-known manufacturing process where a polymer sheet is heated to pliable condition at the forming temperature and stretched into a specific shape in a mould and finally trimmed to obtain a usable product. Thermoforming process is used widely in industry because of its cost-effective manufacturing process. The main objective of this project is to study the effect of the thermoforming process and parameter on the thickness distributions of the thermoforming product by using ANSYS Polyflow simulation. ANSYS Polyflow simulation is used to study the overall thermoforming process to save time and reduce the cost used to produce any prototype product. Mould with different shapes which are corner edge (3mm fillet) and sharp edge are used and simulated to obtain the best thickness distribution on the product. Mould with corner edge (3mm fillet) reduced and distributed the stress more evenly on the product. Therefore, the value of the thickness at the inside corner (critical corner) has been reduced. Grid analysis is performed on the thermoforming product with and without printed circuit. The result showed that the substrate elongated more without the printed circuit on it. The deformation of the substrate with printed circuit embedded on it is much lower. However, the substrate is able to well deform with the printed circuit according to the shape of the mould. Larger area stretch ratio is found at the critical corner and lower sidewall. Higher elongation occurred as the depth of draw increased. Therefore, the thickness distributions are reduced and increased the area stretch ratio as the depth of draw increased. In conclusion, the understanding and technique of thermoforming process on the lighting part has been fully developed.

CHAPTER 1

INTRODUCTION

1.1 BACKGROUND

Thermoforming refers to a process that begins with an extruded sheet of plastic. The process involves heating the plastic sheet to a temperature range where it is soft or malleable. The sheet is then stretched against a cool single-sided mold. When the sheet has cooled to the point where it retains the shape of the mold, it is removed and the excess plastic is trimmed from the formed product. Thermoforming represents a group of sheet-forming processes that includes vacuum forming, drape forming, billow or free bubble forming, mechanical bending, matched-mold forming, billet molding, pressure forming, and twin-sheet forming.[1]. The raw materials used for thermoforming are high impact polystyrene acrylonitrile butadiene styrene (ABS), polypropylene, high-density polyethylene (HDPE) and polycarbonate. The choice of the thermoformed material depends on the use requirements and cost. Figure 1.11 below shows the major steps involved in the thermoforming process from heating to trimming.[2]

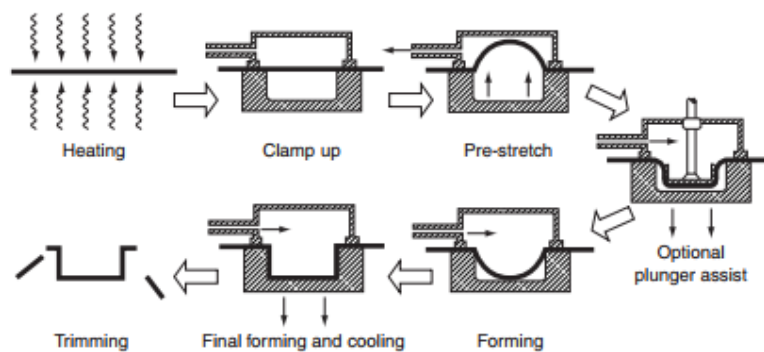


Figure 1.11: Main steps for thermoforming process.[2]

Stretchable electronic circuit is a technology where stretchable electronic devices are embedded onto stretchable substrates such as polyimide, polyethylene terephthalate (PET) and thermoplastic polyurethane (TPU). Stretchable electronic circuit allows 3-D design geometries of both circuits and substrates. This development of stretchable electronic system is capable of absorbing large strains while maintaining electronic functionality. The used of conventional flat rigid assembled printed circuit board (PCB) in the industry become problematic because there is a need to comfortably integrate the circuit on a non-flat surface. Meanwhile, the used flexible circuit and moulded interconnect devices (MID) are time consuming and very expensive to be produced[3]. Figure 1.12 (a) illustrates the 3D-MID circuit which produce more flexible and reliable 3D shapes at a competitive price compared to PCB type flex-rigid technologies. Figure 1.12 (b) shows industrially produced flex-rigid boards which have limitation on freedom of design and random form factors.

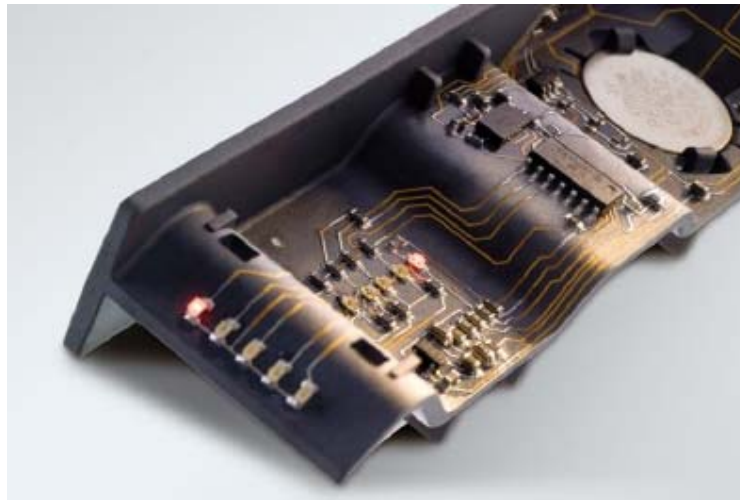


Figure 1.12 (a) : 3D-MID circuit with assembled components.[3]

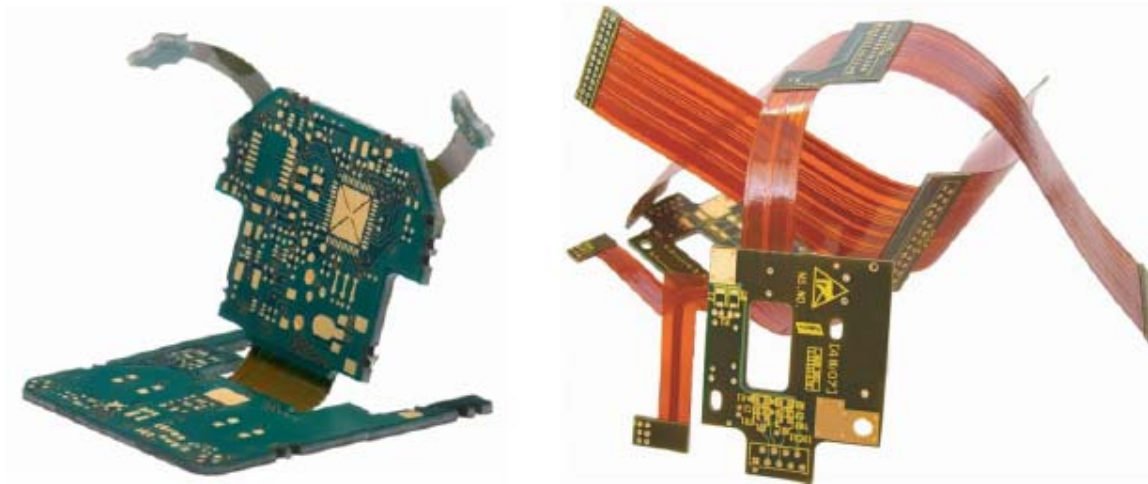


Figure 1.12 (b) : Examples of industrially produced flex-rigid boards (left:Altium), (right:Teknoflex)[3]

As alternative to MID method, printed stretchable circuit is introduced using thermoforming process to manufacture automotive lighting parts. Therefore, certain parameters need to be considered in order to apply the thermoforming process on the stretchable circuit. This new manufacturing process of printed circuit offers a future alternative method in manufacturing the automotive lighting product as it is more cost effective for custom design production.

In this research, simulation of the thermoforming process is performed on the polycarbonate substrate to be transformed into 3-D shape of the lighting part of Proton Saga. The wall thickness distribution and the area stretch ratio of the thermoformed product will be measured to study the effect of thermoforming process on the thermoformed product. The simulation process was conducted according to its parametric study to get the best wall thickness distribution so that stretchable circuit can be implemented on the product. Figure 1.13 (a) and (b) shows the original lighting part of Proton Saga and its Solidworks drawing.

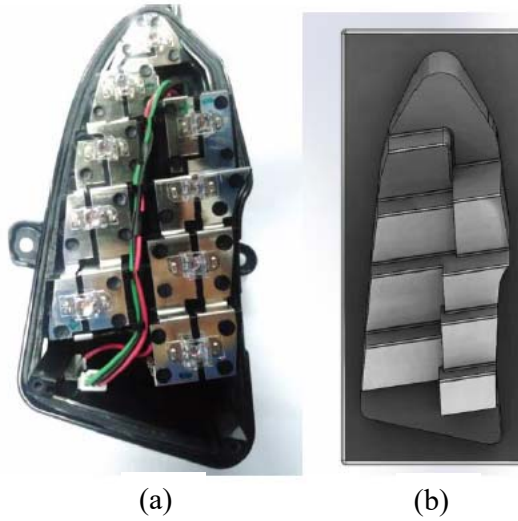


Figure 1.13: (a) The original design of the automotive lighting part (b) 3-D drawing of the original design .[4].

Trial and error methods are used to develop and design new products in the thermoforming industry. This process is time consuming and expensive. Therefore, simulation software such as ANSYS Polyflow is used to develop new thermoforming product. The behavior of the polymers and the wall thickness distribution will be observed during thermoforming simulation process.

1.2 PROBLEM STATEMENT

Currently, moulded interconnect devices (MID) method is used to manufacture the automotive lighting parts. Since this method is using injection molding, laser direct structuring (LDS) and metallization of conductor process, it required a high cost in production due to expensive instrument used such as laser machine. This method is not suitable for custom design production.

Thus, an alternative method which is printed stretchable circuit is introduced using thermoforming process to manufacture automotive lighting. Since the equipment involved in the thermoforming process is low cost when compared to other plastics processing equipment such as injection molding thus by using this alternative method a stretchable circuit can be produced at a reasonable cost on the thermoformed. The tooling and molds can be produced from variety of materials as thermoforming process use low pressure to operate. The simulation of thermoforming process will reduce cost and is time effective to investigate the overall thermoforming process of the thermoformed product so that stretchable circuit can be applied on the thermoformed product.

1.3 OBJECTIVE

The objectives of this research are:

1. To investigate the effect of different shape of mold geometries on the final wall thickness distribution and the area stretch ratio during the thermoforming process,
2. To determine the relationship between wall thickness distribution and the area stretch ratio when different shapes of mould were used during the thermoforming process.

1.4 SCOPE OF WORK

ANSYS Polyflow Blow Molding is used to visualize the performance of the lighting part according to the different geometry of the mold shapes used. It visualizes the behavior of the substrate in terms of area stretch ratio and thickness after deformation according to the shape of mould geometry. The available mould of lighting part of Proton Saga will be modified in term of geometry such as the radius and curve based on certain limit of the parameter so that the thickness distributions on the thermoforming product can be improved.

The simulation of the thermoforming process is done to obtain the best thickness distribution to achieve the best performance for lighting part when the stretchable circuit is embedded on the substrate. The wall thickness distributions from the model were measured and compared to simulation result. The percentage of elongation of the mould with printed circuit and without printed circuit were measured and analyzed.

1.5 THESIS STRUCTURE

The thesis is divided into five chapters. In chapter one, background study, problem statement, objectives and scope of research were briefly discussed.

In chapter two, literature studies on the fundamental studies of the thermoforming process , parametric studies which affect the wall thickness distribution during the thermoforming process, polycarbonate substrate and the detailed of stretchable circuit application were discussed.

Methodology approach in developing a new technique which used the thermoforming in manufacturing of automotive lighting part was discussed. The simulation setup using ANSYS Workbench 16.1 on the thermoforming process of the lighting part has been highlighted in chapter three. The experimental setup and measurement technique were done to get the wall thickness distribution and the material properties of the polycarbonate model of the lighting part.

In chapter four, the effects of parametric study such as mould geometry on the thermoformed product were discussed. The relationship between the final wall thickness distribution and the area stretch ratio were discussed in detail. The experimental and simulation result were compared and discussed further in this chapter

Finally, the objectives made in the beginning were discussed and concluded and the conclusions of the overall thesis with some recommendations or improvements for future work were discussed in chapter five.

CHAPTER 2

LITERATURE REVIEW

2.1 INTRODUCTION

This chapter will discuss on the topics that are related to the thermoforming process, the parameters that affect the thermoforming process, the behavior of the polycarbonate substrate and the simulation of the thermoforming process.

2.2 THERMOFORMING PROCESS

Thermoforming is a process where the heated thermoplastic sheet is deformed and shaped over mould geometry by mechanical, air or vacuum pressure. Thermoforming process is starting from sheet preparation, loading, heating, forming, cooling, unloading and finally trimming[5]. There are many types of thermoforming techniques but the main focus is on vacuum forming. Vacuum-forming is considered as a simplified manufacturing process of thermoforming process. In vacuum forming, the edge-clamped thermoplastic sheet (polycarbonate) is firstly heated to its glass transition temperature and rapidly stretched by a certain pressure into a specific shape of a mold and finally held against the mold by applying vacuum between the mold surface and the sheet until it cools as shown in Figure 2.21[6].

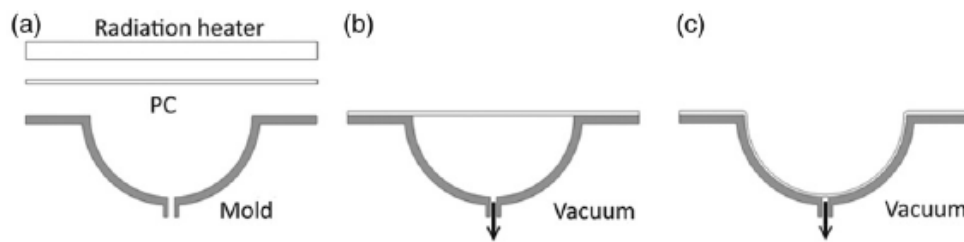


Figure 2.21: Schematic diagram of vacuum-forming process: (a) sheet heating (b) sheet stretching, and (c) sheet cooling.[6]

2.3 PARAMETER EFFECT ON THERMOFORMING PROCESS

Plug assisted thermoforming is a thermoforming process which involved both a mechanical plug and air pressure. Process parameter and material parameter are the two main types of controlling parameter for plug assisted thermoforming. Material parameters include the properties of the sheet, plug, and mold. The material selection will determine the thermal and frictional properties of the contacting surfaces. The design of the plug has been found to have the greatest influence on the quality of the final product. Process parameters include plug speed, plug displacement, plug shape, plug temperature, air pressure, air pressure timing, sheet temperature, and mold temperature. These parameters are adjustable and used to fine tune of wall thickness distribution. The process parameters which shown the greatest effect on the wall thickness distribution include the plug displacement, sheet temperature, plug temperature, and plug shape[7].

Three different plug displacements of 76.5 mm, 81.5 mm, and 86.5 mm were used in the investigation on the wall thickness distribution. Figure 2.31 illustrate the effect of plug displacement on the measured wall thickness distribution.

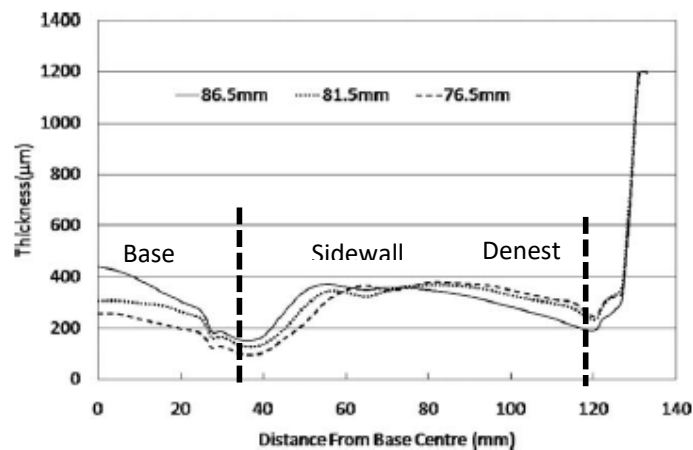


Figure 2.31: The effects of plug displacement on the product wall thickness distribution[7].

The changes of the sheet wall thickness distribution with increasing plug displacement were relatively large from the upper sidewall region into lower sidewall region and base as illustrated in Figure 2.31. This changes were due to the fact that the sheet material drawn downward with the plug has greater travel distance during blowing step when the when the plug displacement decreases. Thus, the material will experience greater thinning.

The material will be peeled downward, away from the plug and onto the mold wall since the blowing pressure is applied from the top surface of the sheet. From Figure 2.32, it is clearly showed that when the plug displacement is decreased, an increased blow-off distance combined with the downwards peeling action will increase the magnitude of stretching in the base region[7].

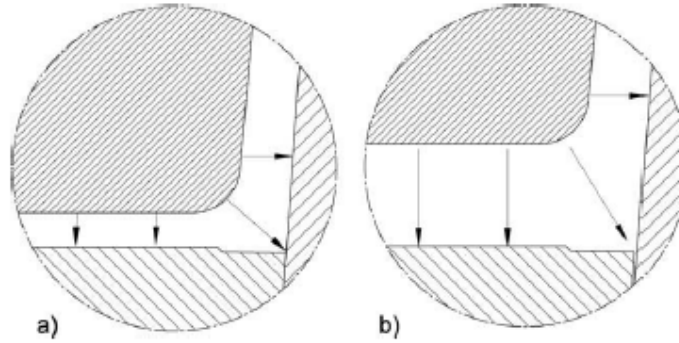


Figure 2.32: Visual representation of plug displacements of (a) 86.5 mm and (b) 76.5 mm showing increased blow-off distance[7].

Three different sheet temperature variations of 120°C, 130°C and 140°C were used in the investigation on the wall thickness distribution. Figure 2.33 shows the effect of sheet temperature variations on the measured wall thickness distribution.

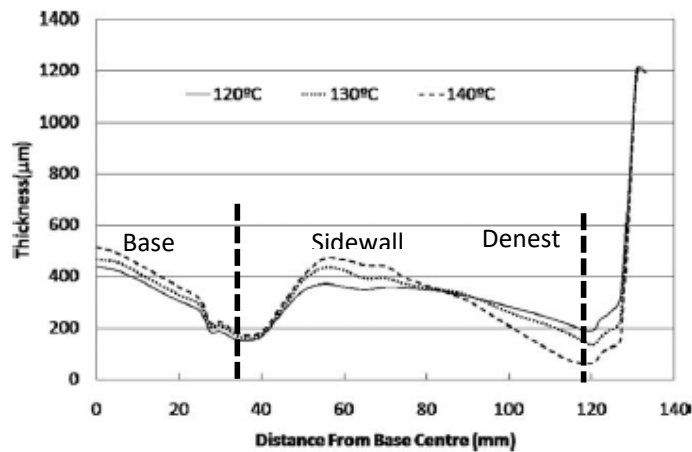


Figure 2.33: The effects of sheet temperature on the product wall thickness distribution[7].

It would be expected that the sheet would be easier to deform at higher temperature. But the drawing actually increases the thicknesses in the base and lower sidewall regions of the product from the very thin denest region. Since the contact friction is highly dependent on the sheet temperature, thus the sheet is sliding less during plug contact creating a thicker base

region during the higher temperature of sheet were used. Therefore, the higher sheet temperature produced thinner denest region which resulting in a very poor mechanical performance of the product. Figure 2.34 shows the microscopy images of the lip and denest regions of the pots formed at 120°C and 140°C. Since the function of the denest is to facilitate stacking, the 140°C pot would perform very poorly[7].

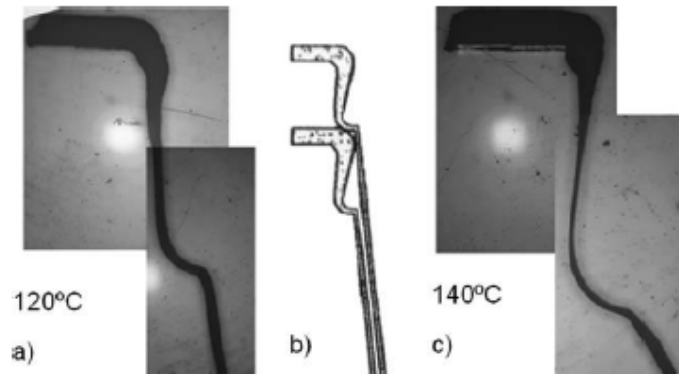


Figure 2.34: Microscopy images (X10 magnification) of the lip and denest regions of pots formed at (a) 120°C and (c) 140°C with (b) stacking[7].

Three different shapes of the plug were included in the investigation since the plug design plays an important role on thermoforming process. The three different shapes of plug used during the investigation were (a) flat bottom, b) blunt, and (c) bullet, as shown in Figure 2.35.

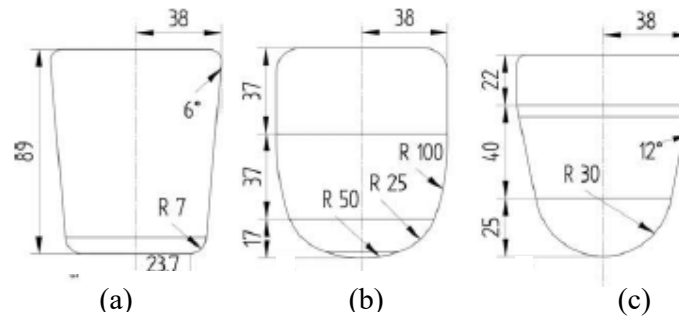


Figure 2.35: (a) Flat bottom (b) blunt, and (c) bullet plug (units in mm)[7].

The wall thickness distribution on the different plug shapes were presented in Figure 2.36.

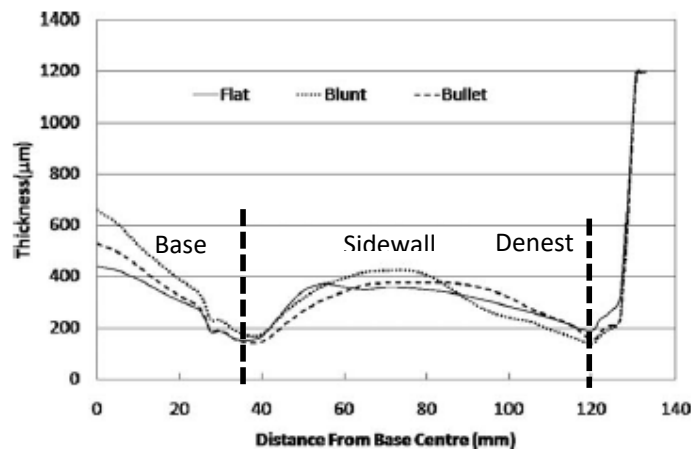
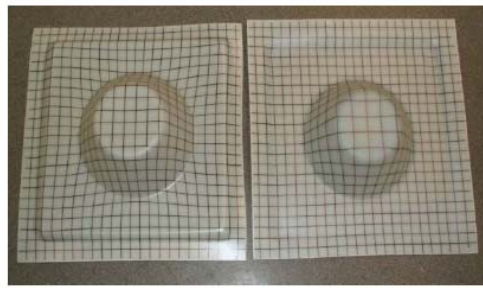


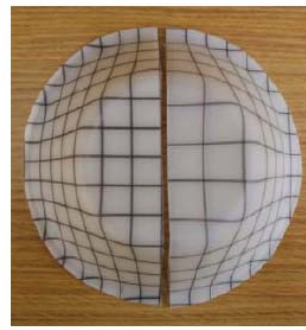
Figure 2.36: The effects of plug shape on the product wall thickness distribution[7].

From Figure 2.36, bullet plug is considered as the most rounded of the design followed by the blunt plug and finally the flat bottom plug. The blunt design created the thickest base and the flat bottom design created the thinnest base while the bullet design was lying in between. Since the contact friction play important role during the process, all plug shapes created relatively thin corner. There would be little extensional slip of the sheet over the flat bottom of the plug in the presence of higher friction and the base of the product would retain considerable thickness. Thus, the rounding of the plug corners will produce a more gradual plug to sheet contact action that pushes the sheet sliding effect further along the distribution which leaves a thicker central base region[7].

The type of mold used (plug or cavity mold) has a huge impact on the distribution of wall thickness variation of the thermoformed product. A pair of molds made of composites (fiberglass and polyester) was created to demonstrate the wall thickness differences between parts produced on a cavity mold and a plug mold. The molds are mounted on a vacuum base which is compatible with the thermoforming equipment in use and the part geometry is nearly identical between mold types. The two sheets to be formed in this test are marked with a 0.5 inch x 0.5 inch grid on each side prior to forming. After the thermoforming process is done, the result between cavity moulded part and plug moulded part is compared. Figure 2.37 illustrates the parts formed by plug mould and cavity mould[5].



(a) plug mould



(b) cavity mould

Figure 2.37: Parts formed by (a) plug mould and (b) cavity mould[5].

Figure 2.38 shows wall thickness distribution of the cavity mould in which the starting sheet thickness was 0.150 inch. The thinnest location of the cavity mould is 0.060 inch which represents 40% of the original thickness.

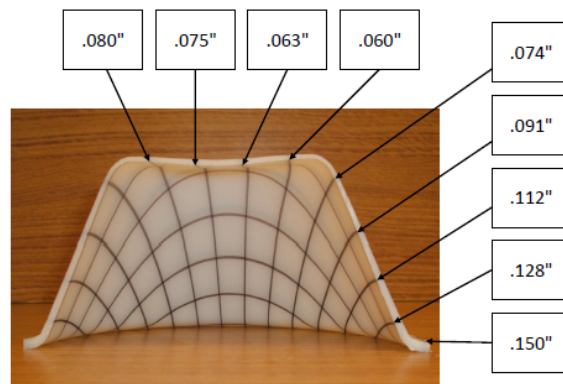


Figure 2.38 : Thickness distribution of part cross section formed by cavity mould[5].

Figure 2.39 shows wall thickness distribution of the plug mould in which the starting sheet thickness was 0.128 inch. The thinnest location of the plug mould is 0.106 inch represents 70.6% of the original thickness.

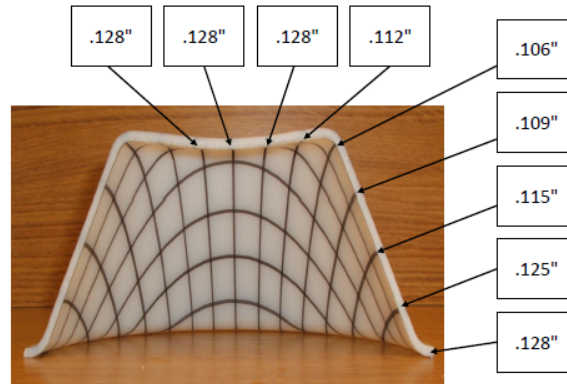


Figure 2.39: Thickness distribution of part cross section formed by plug mould[5].

Therefore, Figure 2.38 clearly shows that the bottom of the cavity molded bowl is very thin due to extreme stretching. While Figure 2.39 illustrates that the bottom of the plug molded bowl is nearly unchanged from the original sheet thickness.

2.4 BEHAVIOUR AND PROPERTIES OF SUBSTRATE MATERIAL

There are two main categories of plastics which are thermoplastics and thermosets. Thermoplastics are materials that can be heated, softened, reformed, and cooled to a solid state repeatedly. Thermosets are the polymers which use heat to cure the material and once cured; they cannot be softened and re-formed. Thus, the plastics used in the thermoforming process are usually thermoplastics. Thermoplastics are characterized by their degree of crystallinity which is amorphous and crystalline or semi-crystalline.

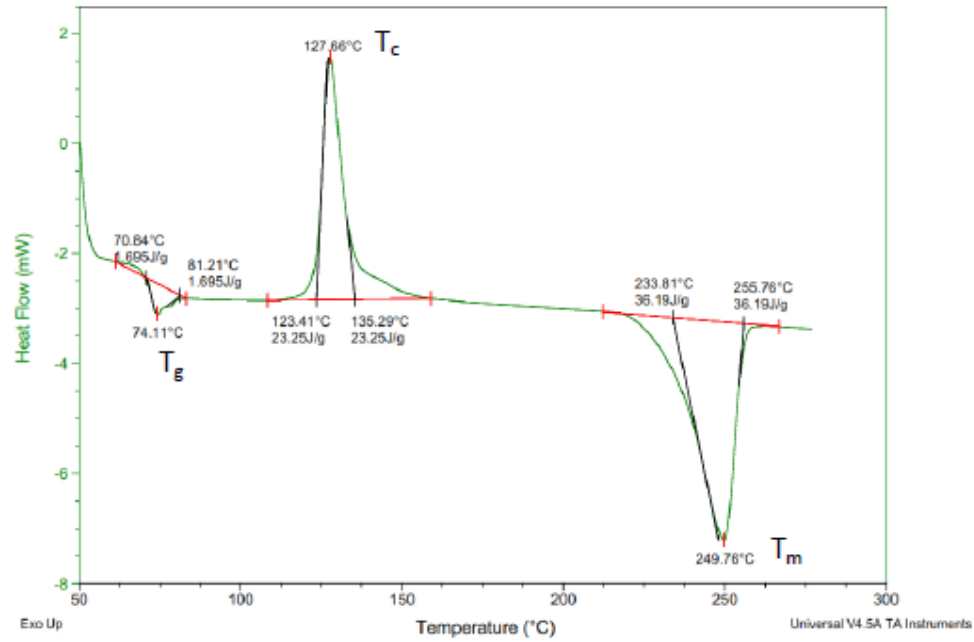
Crystalline refers to a very orderly grouping of molecules rather than a true crystal structure. While amorphous materials lack these orderly regions therefore the term amorphous means “without order. The degree of crystallinity is important to the thermoforming process. Amorphous materials change gradually when heated. These materials will slowly soften when more heat is applied until reached the characteristics of a very viscous liquid. The materials are easier to stretch when more heat is applied. While a crystalline material has a sharp melting point (melting temperature, T_m) therefore, forming only can occur when the material is within about 5 to 10 degrees of the melting temperature. During the thermoforming process, the melting temperature must not be reached because the sheet will rip or fail in the oven.

The thermoplastic materials will undergo physical transition from glassy state to rubbery state when heated. The temperature at which the thermoplastic materials change its phase from glassy state to rubbery state is known as the glass transition temperature, T_g . Polymer that undergoes this transition is known as amorphous polymer such as polycarbonate (PC), ABS, polystyrene, polysulfone, and polyetherimide. The advantages of polycarbonate material are transparency, dimensional stability, flame resistance, high heat distortion temperature, and it is a transparent amorphous polymer which exhibits outstanding physical properties such as impact resistance (almost unbreakable) and excellent clarity.

When polymer undergoes further heating which is the second physical transition from rubbery state to melting state which is known as crystalline or semi-crystalline polymer such as polyethylene, polypropylene, nylon, acetal, polyethersulfone, and polyetheretherketone.

Based on the previous study, the two types of thermoplastics material that had potential to be used in thermoforming process are polyethylene terephthalate (PET) and polycarbonate (PC) due to their excellent thermoforming properties. When PET is heated above the glass transition temperature, it turned opaque due to the spherulitic structure generated by thermal crystallization aggregates of un-oriented polymers[8]. Differential Scanning Calorimetry (DSC-Q20) analysis was used to determine the glass transition temperature, T_g for each substrate to determine a suitable substrate for the thermoforming process.

The PET which known as semi-crystalline material able to achieve glass transition temperature (T_g), crystalline temperature (T_c) and melting temperature (T_m) points when heated at a required temperature. Since PC is an amorphous material, it only achieves the glass transition temperature, T_g [4]. Figure 2.41 (a) and (b) show the DSC scanning result on the temperature of PET and PC.



(a)

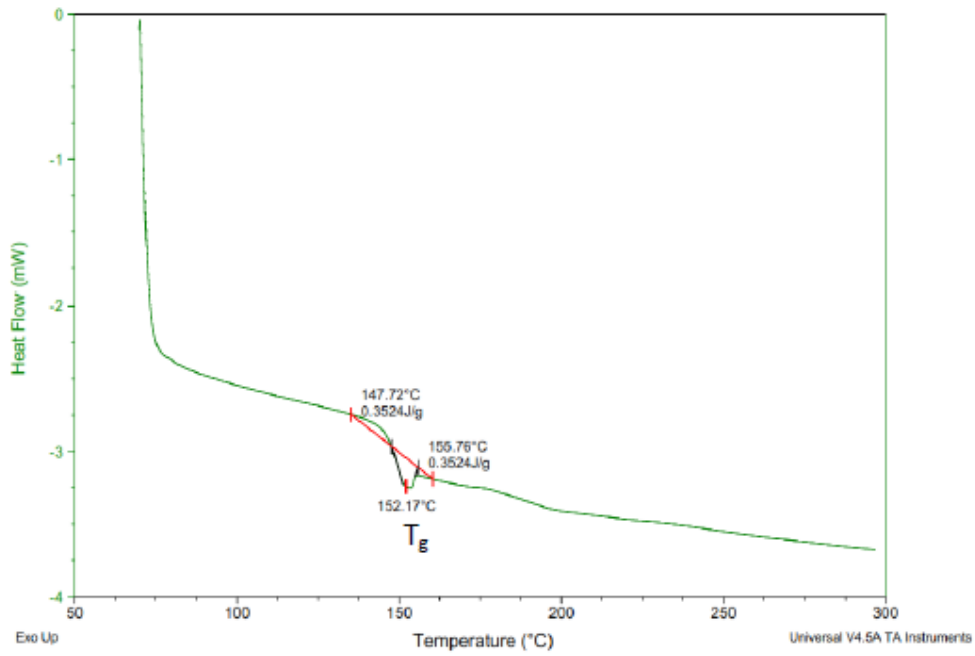


Figure 2.41: DSC scanning result for (a) PET and (b) PC materials[4].

Figure 2.41 (a) shows the first, second and third peaks indicate T_g , T_c and T_m of the PET material while Figure 2.41 (b) illustrates one peak which indicates T_g of the PC material. T_g is important in order to determine the range of temperature for any operation. In the thermoforming process, deformation of the substrate occurred at T_g when the substrate starts

to soften. Excessive heating of the substrate may cause folds, webbing or wrinkles on the thermoformed product.

From the DSC analysis, T_g for PET and PC was approximately 73°C and 150°C respectively. Since the T_g for the PET was below the curing temperature of the adhesives used as interconnect of LED joints at 120°C, PET material will experience critical deformation when heated to 120°C, resulting to the damage of the thermoformed product. PC was the most suitable substrate for the thermoforming process since its T_g is more than the curing temperature[4].

2.5 FINITE ELEMENT SIMULATION OF THERMOFORMING PROCESS

Finite element simulation of the thermoforming process is a relatively new approach for predicting the final wall thickness distribution on the thermoformed parts. From the previous study, the predictions of the thickness distributions are so close to actual measurements as simplifying assumptions were used in developing a numerical model for a complex forming process. Therefore, finite element simulation of thermoforming process has a major impact on the way new parts and processes are designed which could lead to drastic savings in material costs through its design optimization[9].

A thermoforming process simulation of thin polymer films on the non-isothermal viscoelastic model is studied to predict the final thickness distribution of the deformed sheet. The sheet was heated to the forming temperature by infrared radiation during the thermoforming process. Thus, there will be heat transfer during the thermoforming process. Figure 2.51 illustrates the heat transfer mechanism that takes place between the infrared lamps, the polymeric sheet, and the mold during the heating process[10].

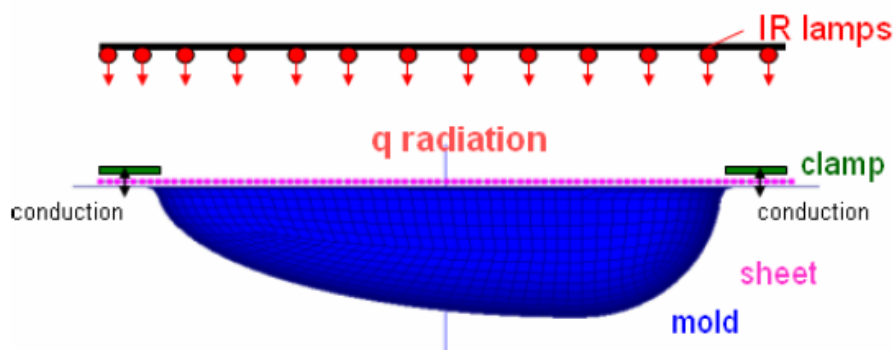


Figure 2.51 : Heat transfer mechanisms[10]

Simulation for this heating process requires accurate modeling of the radiative flux, intercepted and absorbed by the polymeric sheet, the conduction through the thermoplastic sheet, the conduction between the thermoplastic sheet and the mold, and the natural convection from the top and bottom surfaces of the thermoplastic sheet to the surrounding environment.

The temperature of each element of the thermoplastic sheet is known after solving the following heat equation:

$$\rho CV_i \left(\frac{T_i^{t+1} - T_i^t}{\Delta t} \right) = q_{rad,i} + q_{cond,i} + q_{conv,i} \quad (2.51)$$

Where ρ is the density, C is the specific heat capacity, T_i is the temperature of element i , t is the time, Δt is the time step, q_{rad} is the heat flow due to the radiation, q_{cond} is the heat flow due to the conduction and q_{conv} is the heat flow due to the convection.

The simulation of heat transfer from the infrared lamps to the film during the heating stage is transferred by radiation using the following equation:

$$q_{rad} = -\varepsilon_{film} \sigma F S T_{film}^4 + \varepsilon_{lamp} \sigma F S T_{lamp}^4 \quad (2.52)$$

Where ε is the emissivity, σ the Stefan-Boltzmann constant, F the view factor, S the surface area, and T is the temperature.

The heat transfer by conduction between the film and the mold is calculated using the following differential equation:

$$q_{cond} = k_{film} \left(\frac{\partial T}{\partial S} \right)_n S_n \quad (2.53)$$

Where k is the conductivity of the film, S is the contact surface, and T is the temperature.

The heat flow by convection between the film and the surrounding environment is calculated by using the below equation:

$$q_{conv} = hS(T_{air} - T_{film}) \quad (2.54)$$

Where h is the convection coefficient, S is the plate surface area, T_{air} is the air temperature and T_{film} is the surface temperature on the film[10].

The non-linear viscoelastic behavior of polymers was defined by the integral type models. The KBKZ viscoelastic constitutive model was used to handle the behavior of isotropic thermoplastic materials. $M(t, s)$ is the linear viscoelastic memory function as in the following equation:

$$M(t, s, T) = \sum_{k=1}^N \frac{g_k}{\tau_k} e^{(-\frac{t-s}{\tau_k})} \quad (2.55)$$

Where τ_k and g_k are the relaxation times and relaxation modulus coefficient at reference temperature, T_0 .

The temperature dependence of viscosity is expressed by using the William-Landel-Ferry (WLF) equation:

$$\ln[a_T(T)] = -\frac{C_1(T-T_0)}{C_2+T-T_0} \quad (2.56)$$

Where a_T is the shift factor, T is the absolute temperature (calculated by the heating simulation), C_1 and C_2 are the material constants.

This equation is used for $T_g \leq T_0 \leq T_g + 100K$ (T_g is the glass transition temperature). For $T_0 \geq T_g + 100K$, the Arrhenius relation was used:

$$\ln[a_T(T)] = \frac{E_0}{R} \left(\frac{1}{T} - \frac{1}{T_0} \right) \quad (2.57)$$

Where R is the universal gas constant and E_0 is activation energy[10].

2.6 RHEOLOGY TEST

The rheological studies for polymers were done to obtain the viscosity function and dynamic viscoelastic properties of a material. It can be measured continuously when polymers undergo the phase change when the temperature is applied.

From the previous study, ARES rotational rheometer (Rheometric Scientific) was used to measure the complex viscosity and complex modulus. The polycarbonate specimen used was 25mm in diameter. The dynamic viscosity polycarbonate substrate were measured in a parallel-plate fixture (diameter=25 mm) with a gap distance of 1.2 mm. The strain was kept at 10% to ensure linear viscoelasticity. The frequency range used was 0.1-500 rad/s at 230°C. This experiment is done to obtain the viscoelastic properties of polycarbonate such as viscosity, shear rate, storage moduli and loss moduli[10].

Rheological measurements were performed with the Rotational Rheometer (AR-G2) was used to perform rheological measurement by using the plate-plate geometry as illustrated in Figure 2.61(a) and Figure 2.61 (b).

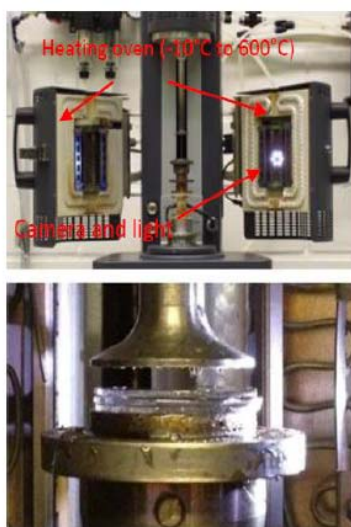


Figure 2.61 (a): AR-G2 (TA-Instruments) rotational rheometer with the used plate-plate geometry[10].

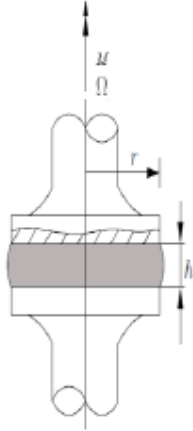
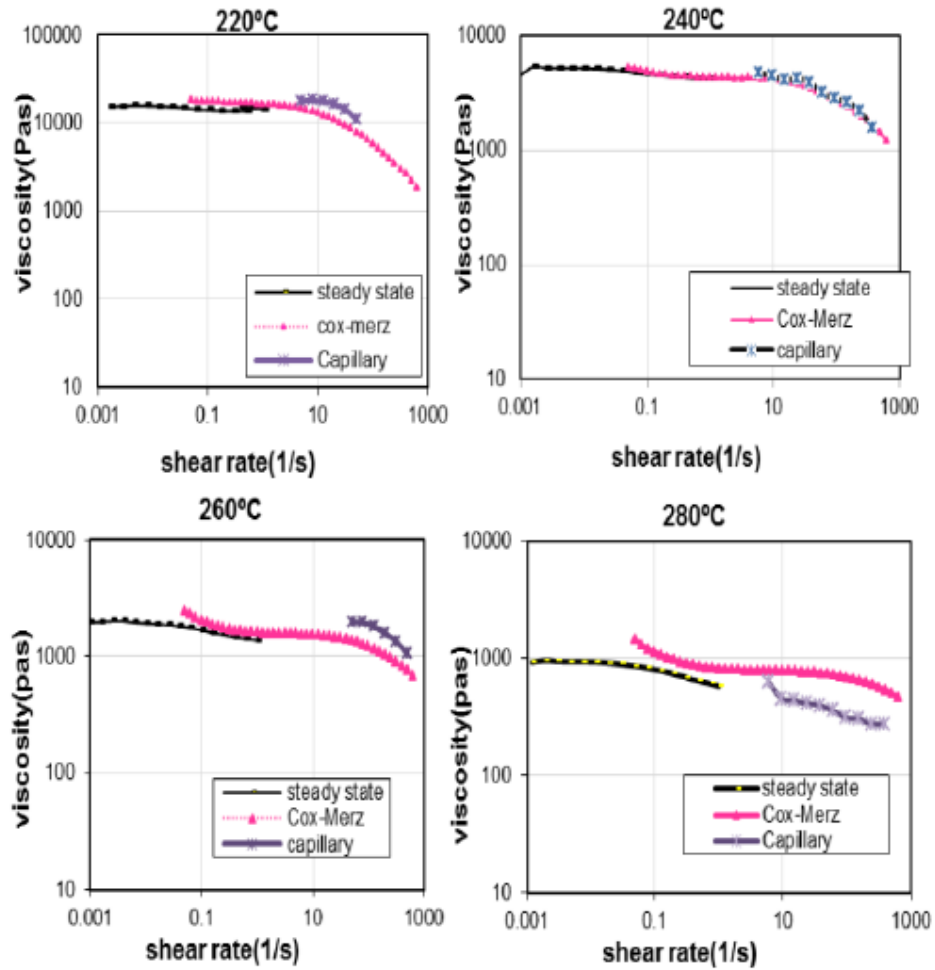


Figure 2.61 (b) : Plate-plate geometry system[10].

Viscoelastic material functions usually measured by using parallel plates. Steady viscosities were computed at different shear rates within range of 0.0001 s^{-1} to 1 s^{-1} as shown in Figures 2.62.



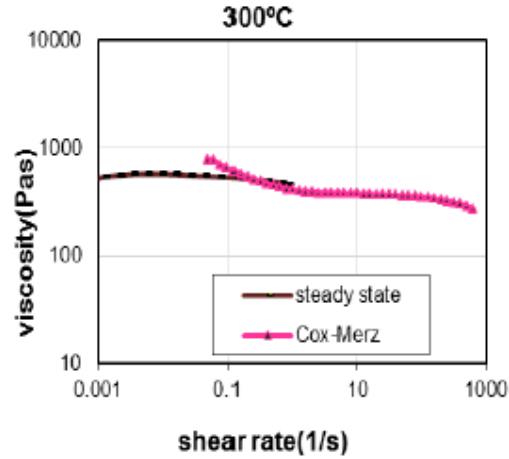


Figure 2.61: Measurements of the shear viscosity of Polycarbonate at a temperature region of 220 °C to 300°C for Steady state, Cox-Merz and Capillary[10].

The same rheometer was used for rheological measurements using oscillatory mode. The frequency of oscillation was varied from 0.01 to 1000 rad/s and the rheological characteristics of polycarbonate were measured at different rate of temperatures from 220-300 °C. The dynamic properties such as storage modulus, G' [Pa], loss modulus, G'' [Pa] and phase angle, δ as a function of angular frequency, ω [rad/s] were measured as illustrated in Figure 2.62 [10].

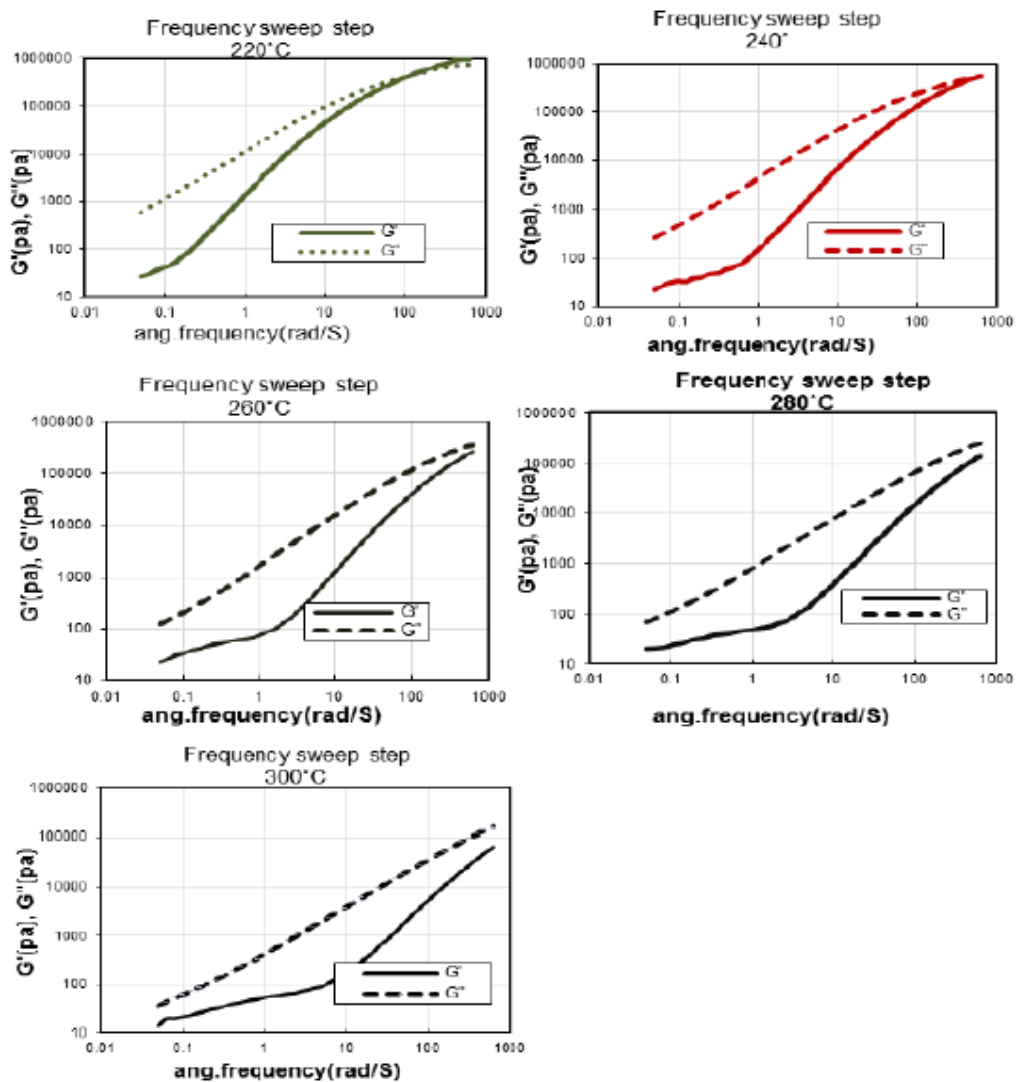


Figure 2.62: Storage and loss modulus for a wide range of frequency, from 220°C to 330°C[10].

2.7 STRETCHABLE ELECTRONIC CIRCUIT

According to journal of “Arbitrarily shaped 2.5D circuits using stretchable interconnections and embedding in thermoplastic polymers”, the developments on thermoformed circuit have started only very recently[3]. The topic of thermoplastic circuits is the focus of study in the thermoplastically deformable circuits for embedded randomly shaped electronics targeting applications in automotive, lighting and consumer electronics industries. Polyethylene terephthalate glycol-modified (PET-G) materials were used as it has the glass transition temperatures around 80°C and were very suitable for thermoforming. Figure 2.71 illustrates the result of a first thermoformed product using a non-optimized design for elastic circuits.

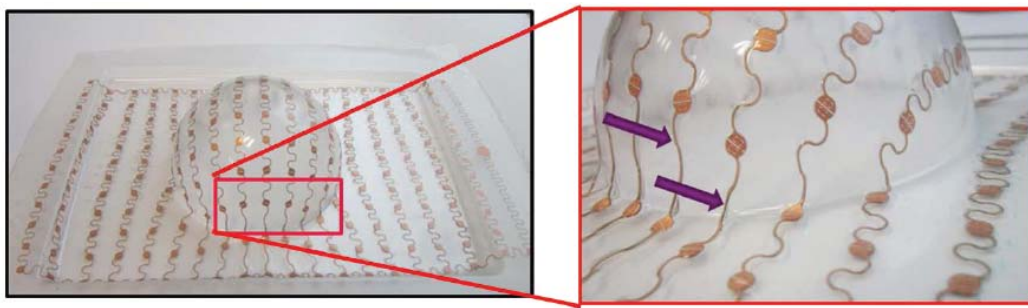


Figure 2.71: First thermoforming experiment, using a non-optimized design, inset (right) shows full extension of meanders.[3]

A flat A4 size circuit was deformed to a 2.5D circuit with a hemispherical shape in the center of the substrate at the forming temperature 120°C. The role of the meanders was to maintain the electrical conduction even under severe deformations. From Figure 2.71, the deformation of the thermoformed product is maximal at the base of the hemisphere and very small at the top. The conductivity of the tracks remained the same after thermoforming even after severe deformations. Based on this experiment, the results show that the thermoplastic deformation of a circuit with assembled components is feasible[3].

2.8 GRID ANALYSIS

Grid analysis was applied to thermoformed product to measure the deformation of the product after the thermoforming process. A study has been conducted on this grid test. Firstly, a grid with square dimensions was printed on the surface of the substrate before the thermoforming process. The extensions of the printed grid were measured after the thermoforming process with the use of a precision imaging measuring system and thickness gauge. Figure 2.71 illustrated the measurement of the printed grid.

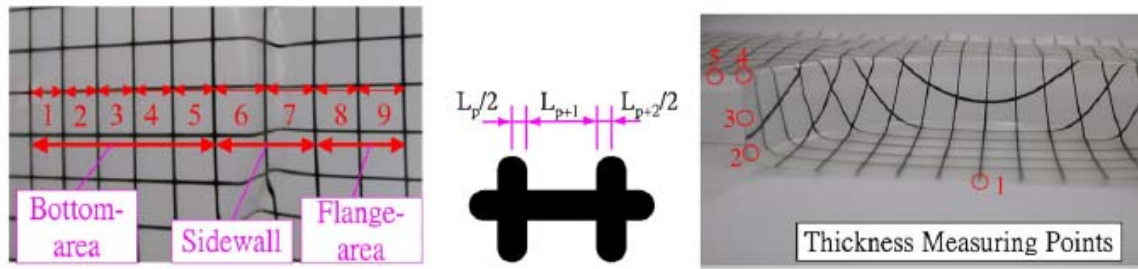


Figure 2.81: (a) Dimensional variation measurement of line segment and (b) thickness distribution of the thermoformed substrate[11].

The initial size of the printed grid was measured before the thermoforming process. After the thermoforming process was done, the final size of the printed grid was measured and the percentage elongation can be calculated. The percentage of elongation was described in the following formula:

$$\delta_L = \frac{L_j - L_i}{L_i} \times 100\% \quad (2.81)$$

Where;

δ_L = percentage of elongation

L_j = measured distance before deformation

L_i = distance after deformation